

Observations of TeV γ -rays from Mrk 421 during Dec. 2005 to Apr. 2006 with the TACTIC telescope

K.K.Yadav^{*}, P.Chandra, A.K.Tickoo, R.C.Rannot, S.Godambe,
M.K.Koul, V.K.Dhar, S.Thoudam, N.Bhatt, S.Bhattacharyya,
K.Chanchalani, H.C.Goyal, R.K.Kaul, M.Kothari, S.Kotwal,
R.Koul, S.Sahayanathan, M.Sharma, K.Venugopal

*Astrophysical Sciences Division, Bhabha Atomic Research Centre.
Mumbai - 400 085, India.*

Abstract

The TACTIC γ -ray telescope has observed Mrk 421 on 66 clear nights from Dec. 07, 2005 to Apr. 30, 2006, totalling ~ 202 hours of on-source observations. Here, we report the detection of flaring activity from the source at ≥ 1 TeV energy and the time-averaged differential γ -ray spectrum in the energy range 1 – 11 TeV for the data taken between Dec. 27, 2005 to Feb. 07, 2006 when the source was in a relatively higher state as compared to the rest of the observation period. Analysis of this data spell, comprising about ~ 97 h reveals the presence of a $\sim 12.0\sigma$ γ -ray signal with daily flux of > 1 Crab unit on several days. A pure power law spectrum with exponent -3.11 ± 0.11 as well as a power law spectrum with an exponential cutoff ($\Gamma = -2.51 \pm 0.26$ and $E_0 = (4.7 \pm 2.1)TeV$) are found to provide reasonable fits to the inferred differential spectrum within statistical uncertainties. We believe that the TeV light curve presented here, for nearly 5 months of extensive coverage, as well as the spectral information at γ -ray energies of > 5 TeV provide a useful input for other groups working in the field of γ -ray astronomy.

Key words: TeV γ -rays, Mrk 421, Observations, Light curve, Energy spectrum

1 Introduction

Markarian 421 is the closest known TeV blazar ($z=0.030$) and was the first extragalactic source detected at TeV energies using imaging atmospheric Cerenkov

^{*} Corresponding author.

Email address: kkyadav@barc.gov.in (K.K.Yadav).

telescopes [1,2]. The source has been regularly monitored by different groups since then [3-9]. It has been seen that the TeV γ -ray emission from Mrk 421 is highly variable with variations of more than one order of magnitude and occasional flaring doubling time of as short as 15 mins [10,11]. Since its detection in the TeV energy range, Mrk 421 has also been the target of several multiwavelength observation campaigns [12-15]. Several groups have also determined the energy spectrum of Mrk 421, both at low average flux levels of < 1 Crab Unit and from intense flares of > 2 Crab Units. The recent results of these studies [4,5,7,16] suggest that the spectrum is compatible with a power law combined with an exponential cutoff. It has also been reported that the spectrum hardens as the flux increases [5,16], either because of an increase in the cutoff energy or a change in the spectral index itself. Differences in the energy spectrum of Mrk 421 and Mrk 501 have also been addressed to understand the γ -ray production mechanisms of these objects and absorption effects at the source or in the intergalactic medium due to interaction of gamma-rays with the extragalactic background photons [17]. A recent review on the observational aspects of TeV γ -ray emission from blazars can be found in [18].

2 Brief description of the TACTIC telescope

The TACTIC (TeV Atmospheric Cerenkov Telescope with Imaging Camera) γ -ray telescope has been set up at Mt. Abu (24.6° N, 72.7° E, 1300m asl), India for studying emission of TeV γ -rays from celestial sources. The telescope deploys a F/1 type tracking light collector of ~ 9.5 m² area, made up of 34 x 0.6 m diameter, front-coated spherical glass facets which have been prealigned to produce an on-axis spot of $\sim 0.3^\circ$ diameter at the focal plane. The telescope uses a 349-pixel photomultiplier tube (ETL 9083UVB) -based imaging camera with a uniform pixel resolution of $\sim 0.3^\circ$ and a field-of-view of $\sim 6^\circ \times 6^\circ$ to record images of atmospheric Cerenkov events. The present data has been collected with inner 225 pixels (15×15 matrix) of the full imaging camera. The innermost 121 pixels (11×11 matrix) are used for generating the event trigger, based on the NNP (Nearest Neighbour Pairs) topological logic [19], by demanding a signal ≥ 25 pe for the 2 pixels which participate in the trigger generation. Whenever the single channel rate of any two or more pixels in the trigger region goes outside the preset operational band (5 Hz-100 Hz), it is automatically restored to within the prescribed range by appropriately adjusting the high voltage of the pixels [20]. The resulting change in the photomultiplier (PMT) gain is monitored by repeatedly flashing a blue LED, placed at a distance of ~ 1.5 m from the camera. The advantages of using such a scheme are that in addition to providing control over chance coincidence triggers, it also ensures safe operation of PMTs with typical anode currents of ≤ 3 μ A. The back-end signal processing hardware of the telescope is based on medium channel density NIM and CAMAC modules developed inhouse. The data acquisition and control system of the telescope [21] has been designed around a network of PCs running

the QNX (version 4.25) real-time operating system. The triggered events are digitized by CAMAC based 12-bit Charge to Digital Converters (CDC) which have a full scale range of 600 pC. The telescope has a pointing and tracking accuracy of better than ± 3 arc-minutes. The tracking accuracy is checked on a regular basis with so called "point runs", where an optical star having its declination close to that of the candidate γ -ray source is tracked continuously for about 5 hours. The point run calibration data (corrected zenith and azimuth angle of the telescope when the star image is centered) are then incorporated in the telescope drive system software so that appropriate corrections can be applied directly in real time while tracking a candidate γ -ray source.

Operating at γ -ray threshold energy of ~ 1.2 TeV, the telescope records a cosmic ray event rate of ~ 2.0 Hz at a typical zenith angle of 15° . The telescope has a 5σ sensitivity of detecting Crab Nebula in 25 hours of observation time and has so far detected γ -ray emission from the Crab Nebula, Mrk 421 and Mrk 501. Some of the results obtained on various candidate γ -ray sources are discussed in [22–24].

3 Observations and data analysis

Using the TACTIC imaging telescope, Mrk 421 was observed for ~ 202 h between Dec. 07, 2005 to Apr. 30, 2006. Only ~ 30 h of data was recorded in the off-source direction in order to maximize the on-source observation time and to improve the chances of recording possible flaring activity from the source. The total on-source data has been divided into 6 spells, where each spell corresponds to one lunation period. The zenith angle of the observations was $\leq 45^\circ$. The general quality of the recorded data was checked by referring to the sky condition log and compatibility of the prompt and chance coincidence rates with Poissonian statistics. The imaging data recorded by the telescope was corrected for inter-pixel gain variation and then subjected to the standard two-level image 'cleaning' procedure [25] with picture and boundary thresholds of 6.5σ and 3.0σ , respectively. The image cleaning threshold levels were first optimized on the Crab data and then applied to the Mrk 421 data. The clean Cherenkov images were characterized by calculating their standard image parameters like LENGTH, WIDTH, DISTANCE, ALPHA, SIZE and FRAC2 [26,27]. The standard Dynamic Supercuts [28] procedure was then used to separate γ -ray like images from the huge background of cosmic rays. The γ -ray selection criteria (Table 1) used in the analysis have been obtained on the basis of dedicated Monte Carlo simulations carried out for the TACTIC telescope. The cuts have also been validated further by applying them to the Crab Nebula data collected by the telescope.

Table 1

Dynamic Supercuts selection criteria used for analyzing the TACTIC data

Parameter	Cut Values
LENGTH (L)	$0.11^\circ \leq L \leq (0.235 + 0.0265 \times \ln S)^\circ$
WIDTH (W)	$0.06^\circ \leq W \leq (0.085 + 0.0120 \times \ln S)^\circ$
DISTANCE (D)	$0.52^\circ \leq D \leq 1.27^\circ \cos^{0.88}\theta$;($\theta \equiv$ zenith ang.)
SIZE (S)	$S \geq 450d.c$;(6.5 digital counts \equiv 1.0 pe)
ALPHA (α)	$\alpha \leq 18^\circ$
FRAC2 (F2)	$F2 \geq 0.35$

4 Results – Alpha plot analysis and light curve

A well established procedure to extract the γ -ray signal from the cosmic ray background using single imaging telescope is to plot the frequency distribution of ALPHA parameter (defined as the the angle between the major axis of the image and the line between the image centroid and camera center) of shape and DISTANCE selected events. This distribution is expected to be flat for the isotropic background of cosmic events. For γ -rays, coming from a point source, the distribution is expected to show a peak at smaller α values. Defining $\alpha \leq 18^\circ$ as the γ -ray domain and $27^\circ \leq \alpha \leq 81^\circ$ as the background region, the number of γ -ray events is then calculated by subtracting the expected number of background events (calculated on the basis of background region) from the γ -ray domain events. Estimating the expected background level in the γ -domain by following this approach is well known [29] and has been used quite extensively by other groups when equal amount of off-source data is not available. However, we have also validated this method for the TACTIC telescope by using separate off-source data on a regular basis and the α distribution of this data in range $\alpha \leq 81^\circ$ is in good agreement with the expected flat distribution. The significance of the excess events has been finally calculated by using the maximum likelihood ratio method of Li & Ma [30].

In order to test the validity of the data analysis chain and, in particular, the energy estimation procedure, we have first analyzed the Crab Nebula data collected by the TACTIC imaging telescope for ~ 101.44 h during Nov. 10, 2005 - Jan. 30, 2006. The events selected after using the Dynamic Supercuts procedure (Table 1) yield an excess of $\sim (839 \pm 89)$ γ -ray events with a statistical significance of $\sim 9.64\sigma$. The corresponding average γ -ray rate turns out to be $\sim (8.27 \pm 0.88)\text{h}^{-1}$. The same data sample has been analyzed again after restricting the zenith angle of the observations to $15^\circ - 45^\circ$ (similar to the zenith angle range which Mrk 421 would cover) so that the resulting γ -ray rate can be designated as a reference of 1 Crab Unit (CU) while interpreting the Mrk 421 data. The analysis yields an excess of $\sim (598 \pm 69)$ γ -ray events in an observation time of ~ 63.33 h with a corresponding γ -ray rate of $\sim (9.44 \pm 1.09)\text{h}^{-1}$, leading to the conversion: $1 \text{ CU} \equiv (9.44 \pm 1.09)\text{h}^{-1}$. While

one would have expected this rate to decrease because of increase in the threshold energy of the telescope at higher zenith angles, the reason behind this increase is the superior γ -ray acceptance of Dynamic Supercuts at higher zenith angles which overcompensates the threshold change effect.

In the case of Mrk 421, we have first analyzed the data for each spell separately. Furthermore, it has also been ensured that the data on both sources (Crab and Mrk 421) are subjected to exactly similar analysis procedures to avoid any source dependent bias while determining the energy spectrum of Mrk 421. The results of the spell wise analysis are presented in Table 2. An examination of this table clearly indicates that Mrk 421 was most active during spell 2 and spell 3 observations. Fig.

Table 2

Detailed Spell wise analysis report of Mrk 421 data

Spell	Obs. time (hrs.)	γ -ray events	γ -ray rate (h^{-1})	Signifi- cance(σ)	χ^2 /dof ($27^\circ \leq \alpha \leq 81^\circ$)	Prob
I	9.24	9 ± 25	0.97 ± 2.67	0.37	2.97 /5	0.705
II	35.71	275 ± 49	7.70 ± 1.37	5.79	5.77 /5	0.329
III	61.53	676 ± 66	10.99 ± 1.07	10.64	8.57 /5	0.127
IV	34.54	91 ± 47	2.64 ± 1.37	1.94	5.10 /5	0.404
V	31.14	61 ± 38	1.96 ± 1.23	1.61	2.44 /5	0.785
VI	29.55	123 ± 33	4.16 ± 1.11	3.86	3.01 /5	0.698
All data	201.72	1236 ± 110	6.13 ± 0.55	11.49	4.57 /5	0.471
II +III	97.24	951 ± 82	9.78 ± 0.84	12.00	5.00 /5	0.416

1a gives the α -distribution when all the data collected for ~ 201.72 h (Dec. 07, 2005 - Apr. 30, 2006, spell 1 to spell 6) is analysed together. The total data yields an excess of $\sim (1236 \pm 110)$ γ -ray events with a statistical significance of $\sim 11.49\sigma$. Fig. 1b gives the corresponding α -distribution for ~ 29.65 h of off-source data. The procedure for estimating the expected background in the γ -domain by using the background region is also consistent with the results from the off-source alpha plot (Fig.1b), when its γ -ray domain events ($\alpha \leq 18^\circ$ events) are appropriately scaled up (to account for the difference in the on-source and off-source observation time) and compared with the γ -ray domain events of Fig.1a. The results of this calculation yield a value of $\sim (8320 \pm 238)$ events for the background level which is in close agreement with the value of $\sim (8171 \pm 52)$ events obtained when background region of Fig.1a is used itself. It is worth mentioning that χ^2/dof of the background region (indicated by column 5 of Table 2) is also consistent with the assumption that the background region is flat and thus can be reliably used for estimating the background level in the γ -domain.

The full light curve of Mrk 421 as recorded by the TACTIC imaging telescope is

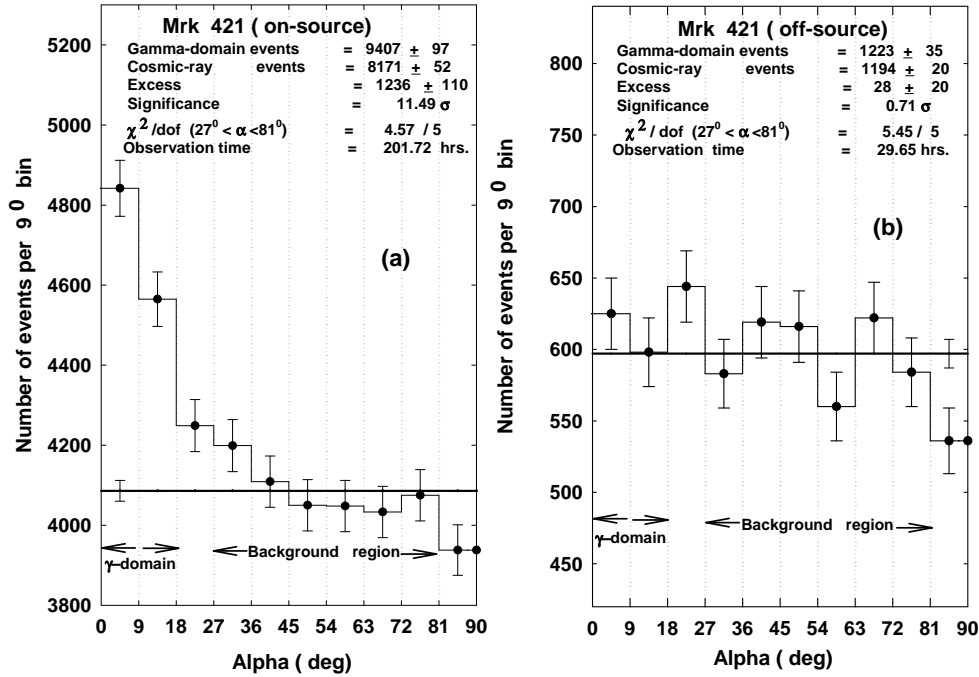


Fig. 1. (a) On-source Alpha plot for Mrk 421 when all the data collected between Dec. 07, 2005 - Apr. 30, 2006 for ~ 201.72 h is analysed. (b) Off-source Alpha plot for ~ 29.65 hrs. of observation time. The horizontal lines in these figures indicate the expected background in the γ -domain obtained by using the background region ($27^\circ \leq \alpha \leq 81^\circ$).

shown in Fig.2a, where daily rates have been plotted as a function of modified Julian date. The corresponding light curve showing the daily average count rate in the 2-10 keV energy band as determined by RXTE/ASM [31] is shown in Fig. 2b. Since the ASM observations were not simultaneous with the observations taken with the TACTIC telescope, a detailed correlation analysis is rather difficult. We have also examined day-to-day flux variability in the TeV light curve of the source for spell 2 and spell 3 data. The results indicate that we cannot claim any statistically significant flux variation on a nightly basis because of rather large error bars.

5 Monte Carlo simulations for energy reconstruction of γ -rays

The Monte Carlo simulation data used for developing a procedure for γ -ray event selection and energy reconstruction of γ -rays are based on the CORSIKA (version 5.6211) air-shower simulation code [32]. The simulated data-base for γ -ray showers uses about 34000 showers in the energy range 0.2-20 TeV with an impact parameter of 5-250m. These showers have been generated at 5 different zenith angles ($\theta = 5^\circ, 15^\circ, 25^\circ, 35^\circ$ and 45°). Furthermore, a data-base of about 39000 proton initiated showers in the energy range 0.4-40 TeV, distributed isotropically within a

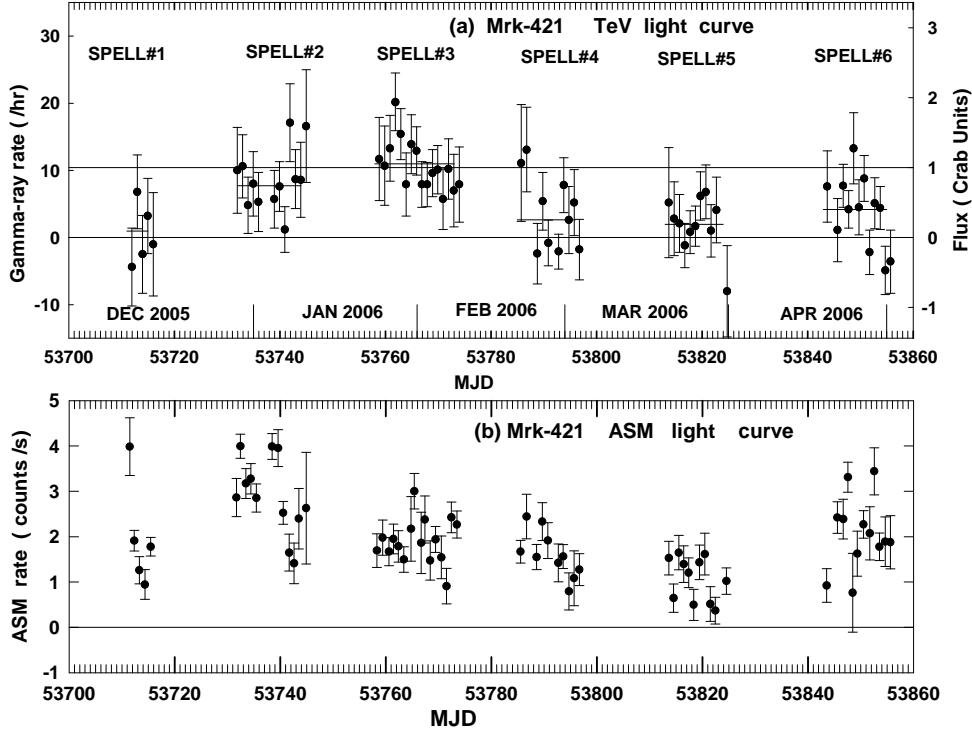


Fig. 2. (a) Light curve for Mrk 421 as recorded by the TACTIC imaging telescope Dec. 07, 2005 - Apr. 30, 2006 for a total observation time of ~ 201.72 h. The horizontal lines marked in between various flux points indicate the spell wise average γ -ray rate. (b) Daily plot of the average count rate in the 2-10 keV energy range as determined by RXTE/ASM X-ray detector

field-of-view $6^\circ \times 6^\circ$, have also been generated for studying the gamma/hadron separation capability of Dynamic Supercuts and confirming the matching of experimental and simulated image parameter distributions. A supplementary code has been developed for the ray tracing of the Cerenkov photons [33] and also to take into account the wavelength dependent atmospheric absorption, the spectral response of the PMTs and the reflection coefficient of mirror facets and light cones. The Cerenkov photon data-base, consisting of number of photoelectrons registered by each pixel, has been subjected to noise injection, trigger condition check and image cleaning. The resulting two dimensional 'clean' Cerenkov image of each triggered event is then used to determine various image parameters. The same simulation data base has also been used, as per the well known standard procedure [28], for calculating the effective area of γ -rays as a function of energy and zenith angle and, also the γ -ray retention factors when Dynamic Supercuts are applied to the simulated data. Here, we present only the details of our energy reconstruction procedure which we believe has been attempted for the first time.

Given the inherent power of ANN (Artificial Neural Network) to effectively handle the multivariate data fitting, we have developed an ANN-based energy estimation procedure for determining the energy spectrum of a candidate γ -ray source. An

ANN is a non-linear statistical data modeling tool which can be used to model complex relationships between inputs and outputs. The tool can be applied to problems like function approximation or regression analysis (similar to what is being attempted here), classification (pattern recognition) etc. Although not for energy estimation, the idea of applying ANN to imaging telescope data was attempted for the first time by Reynolds and Fegan [34]. While a detailed description of ANN methodology can be found in [34,35], we will only present here the main steps taken by us to ensure reliability of end results.

The γ -ray energy reconstruction with a single imaging telescope, in general, is a function of image SIZE, DISTANCE and zenith angle. The procedure followed by us uses a 3:30:1 (i.e 3 nodes in the input layer, 30 nodes in hidden layer and 1 node in the output layer) configuration of the ANN with resilient back propagation training algorithm [36] to estimate the energy of a γ -ray like event on the basis of its image SIZE, DISTANCE and zenith angle. The training and testing of the ANN was done in accordance with the standard procedure of dividing the data base into two parts so that one part could be used for the training and the remaining for testing. We used about 10,000 events out of a total of 34000 parameterized γ -ray images for training. The 3 nodes in the input layer correspond to zenith angle, SIZE and DISTANCE, while the 1 node in the output layer represents the expected energy (in TeV) of the event. In order to make ANN training easier and to smoothen inherent event to event fluctuations, we first calculated the $\langle \text{SIZE} \rangle$ and $\langle \text{DISTANCE} \rangle$ of the training data sample of 10000 images by clubbing together showers of a particular energy in various core distance bins with each bin having a size of 40m. Once satisfactory training of the ANN was achieved, the corresponding ANN generated weight-file was then used as a part of the main data analysis program so that the energy of a γ -ray like event could be predicted without using the ANN software package. Rigorous checks were also performed to ensure that Network did not become "over-trained" and the configuration used was properly optimized with respect to number of iterations and number of nodes in the hidden layer. Optimization of the network was done by monitoring the RMS error while training the ANN. The optimized configuration (3:20:1 with 5000 iterations) yielded a final RMS error of ~ 0.027 which reduced only marginally when the number of nodes in the hidden layer or the number of iterations were increased further.

A plot of energy reconstruction error obtained for test data sample of 24000 parameterized images is shown in Fig.3a. This plot has been obtained by testing the ANN with individual parameterized images at different energies within 5° - 45° zenith angle range. Denoting the estimated energy by E_{ANN} and the actual energy used during Monte Carlo simulations by E_{MC} , Fig. 3b shows the frequency distribution of $(\ln(E_{ANN}/E_{MC}))$ for all events shown in Fig.3a alongwith a Gaussian fit. Having a value of $\sigma(\ln E) \sim 28.4\%$ (Fig.3b), directly implies that the procedure should allow us to retain $\sim 84\%$ γ -rays in most of the energy bins from 1 – 20 TeV, if 6 bins per energy decade (i.e $\sigma(\ln E)$) of $\sim 40\%$ are used for determining the energy spectrum of a candidate γ -ray source. The performance of the ANN-based energy

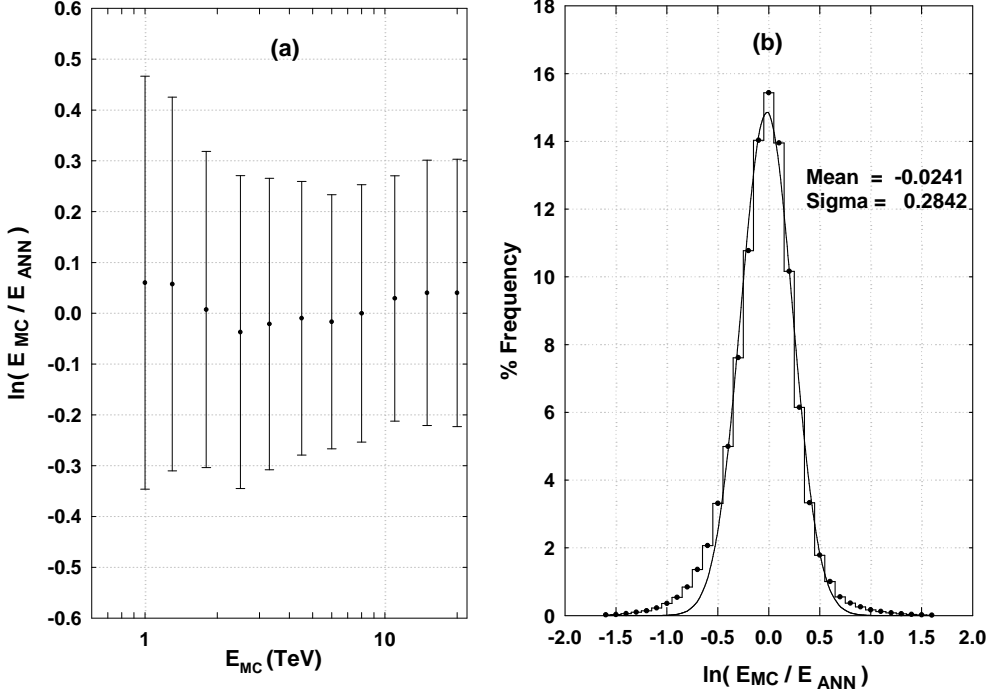


Fig. 3. (a) Error in the energy resolution function ($\ln(E_{ANN}/E_{MC})$) as a function of the energy of the γ - rays for the simulated showers generated within 5° - 45° zenith angle range. (b) Frequency distribution of ($\ln(E_{ANN}/E_{MC})$) for all events shown in Fig.1a along with a Gaussian fit.

reconstruction procedure was also compared with the results obtained from the linear least square fitting method. This method yielded a $\sigma(\ln E)$ of $\sim 35.4\%$. It is also worth mentioning here that the new ANN-based energy reconstruction method used here, apart from yielding a lower $\sigma(\ln E)$ of $\sim 28.4\%$ as compared to $\sigma(\ln E)$ of $\sim 36\%$ reported by the Whipple group [28], has the added advantage that it considers zenith angle dependence of SIZE and DISTANCE parameters as well. The procedure thus allows data collection over a much wider zenith angle range as against a coverage of upto 35° in case the zenith angle dependence is to be ignored.

6 Energy spectrum of Mrk 421

The differential photon flux per energy bin has been computed using the formula

$$\frac{d\Phi}{dE}(E_i) = \frac{\Delta N_i}{\Delta E_i \sum_{j=1}^5 A_{i,j} \eta_{i,j} T_j} \quad (1)$$

where ΔN_i and $d\Phi(E_i)/dE$ are the number of events and the differential flux at energy E_i , measured in the i th energy bin ΔE_i and over the zenith angle range of 0° - 45° , respectively. T_j is the observation time in the j th zenith angle bin with corresponding energy-dependent effective area ($A_{i,j}$) and γ -ray acceptance ($\eta_{i,j}$). The 5 zenith angle bins ($j=1-5$) used are 0° - 10° , 10° - 20° , 20° - 30° , 30° - 40° and 40° - 50° with simulation data available at 5° , 15° , 25° , 35° and 45° . The number of γ -ray events (ΔN_i) in a particular energy bin is calculated by subtracting the expected number of background events, from the γ -ray domain events.

In order to test the validity of the energy estimation procedure, we first used Crab Nebula data collected by the TACTIC imaging telescope for ~ 101.44 h between Nov. 10, 2005 - Jan. 30, 2006. The γ -ray differential spectrum obtained after applying the Dynamic Supercuts and appropriate values of effective collection area and γ -ray acceptance efficiency (along with their energy and zenith angle dependence) is shown in Fig.4a. While determining the energy spectrum, we used the excess noise factor method for converting the image size in CDC counts to number of photoelectrons. The analysis of relative calibration data yields a value of $1\text{pe} \cong (6.5 \pm 1.2)$ CDC for this when an average value of ~ 1.7 is used for excess noise factor of the photomultiplier tubes. The differential energy spectrum of the Crab Nebula shown in Fig.4a is a power law fit ($d\Phi/dE = f_0 E^{-\Gamma}$) with $f_0 = (2.74 \pm 0.19) \times 10^{-11} \text{cm}^{-2} \text{s}^{-1} \text{TeV}^{-1}$ and $\Gamma = 2.65 \pm 0.06$. The fit has a $\chi^2/dof = 0.53/6$ with a corresponding probability of 0.997. The errors in the flux constant and the spectral index are standard errors. Excellent matching of this spectrum with that obtained by the Whipple and HEGRA groups [37,38] reassures that the procedure followed by us for obtaining the energy spectrum of a γ -ray source is quite reliable.

Turning to Mrk 421, since we know now that the source was in a high state during spell 2 and spell 3 observations, we have used this data alone to determine the time averaged energy spectrum of Mrk 421. Fig.4b shows the differential energy spectrum after applying the Dynamic Supercuts to the combined data of spell 2 and spell 3. A power law fit to the data ($d\Phi/dE = f_0 E^{-\Gamma}$) in the energy range 1-11 TeV yields $f_0 = (4.66 \pm 0.46) \times 10^{-11} \text{cm}^{-2} \text{s}^{-1} \text{TeV}^{-1}$ and $\Gamma = 3.11 \pm 0.11$ with a $\chi^2/dof = 2.45/5$ (probability = 0.78). A power law with an exponential cutoff ($d\Phi/dE = f_0 E^{-\Gamma} \exp(-E/E_0)$) was also tried and the results yield the following parameters of the fit $f_0 = (4.88 \pm 0.38) \times 10^{-11} \text{cm}^{-2} \text{s}^{-1} \text{TeV}^{-1}$, $\Gamma = 2.51 \pm 0.26$ and $E_0 = (4.7 \pm 2.1) \text{TeV}$ with a $\chi^2/dof = 0.88/4$ (probability = 0.93). The errors in the flux constant, the spectral index and cutoff energy are again standard errors. While work on understanding the telescope systematics is still in progress, our preliminary estimates for the Crab Nebula spectrum indicate that the systematic errors in flux and the spectral index are $< \pm 40\%$ and $< \pm 0.42$, respectively.

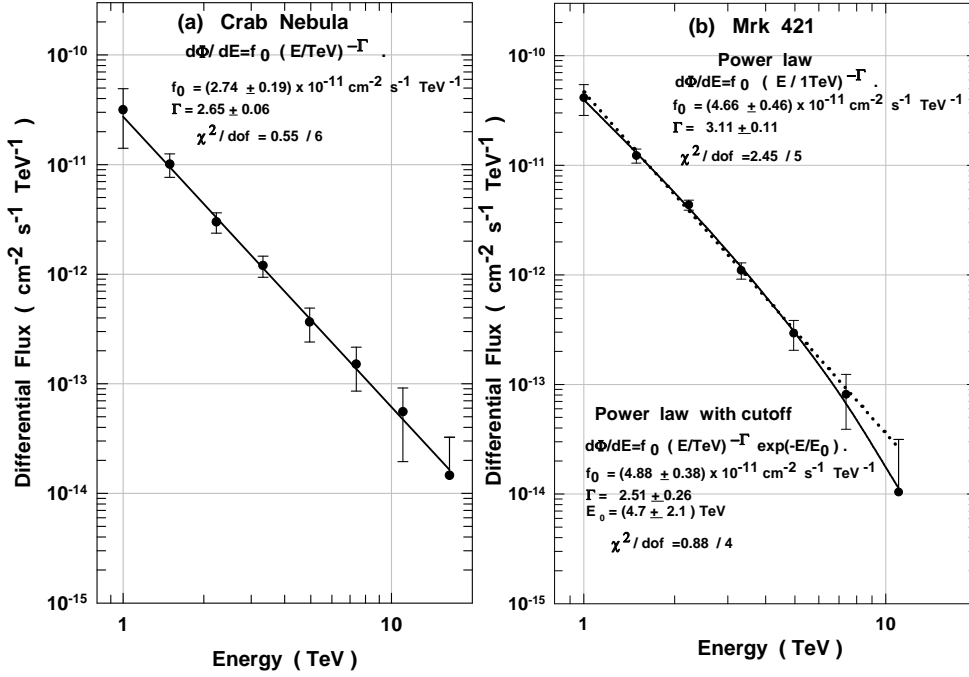


Fig. 4. The differential energy spectrum of the Crab Nebula as measured by the TACTIC telescope. (b) Differential energy spectrum of Mrk 421 for the data collected between Dec. 27, 2005 - Feb. 07, 2006 when the source was in a high state.

7 Discussion and Conclusions

The observations of Mrk 421 carried out with the TACTIC imaging telescope at γ -ray energies of ≥ 1.2 TeV clearly indicate that the source was in a high state during Dec. 27, 2005 to Jan. 09, 2006 and Jan. 23, 2006 to Feb. 07, 2006 at a combined average flux of $\sim(1.04 \pm 0.14)\text{CU}$. It is worth mentioning here that the preliminary results of the Whipple group [39] also indicate that the source was in a high state during the period of their observations from Dec. 27, 2005 - Jan. 07, 2006 and Jan. 23, 2006 - Feb. 03, 2006. Furthermore, our results for spell 5 (Mar. 19, 2006 to Mar. 30, 2006) are also consistent with the Whipple observations from Mar. 23, 2006 to Apr. 04, 2006 when the source was seen to flare at a lower flux level. These observations clearly indicate that, despite difference in the observation time between the two telescope systems, Mrk 421 was observed to be in a high state by both the systems for a prolonged duration, somewhat similar to the flaring episodes during Jan.-Feb., 2001 and Apr.- May, 2004.

The energy spectrum of Mrk 421 as measured by the TACTIC imaging telescope in the energy region 1-11 TeV is compatible with both a pure power law fit with an exponent of $\Gamma = 3.11 \pm 0.11$ ($\chi^2/dof = 2.45/5$; probability = 0.78) and a power law with an exponential cut off with $\Gamma = 2.51 \pm 0.26$ and $E_0 = (4.7 \pm 2.1)\text{TeV}$

($\chi^2/dof = 0.88/4$; probability=0.93). However, a systematic deviation from a pure power law, although not statistically very significant, is evident in Fig.4b at the energy values of 7.4 TeV and 11.0 TeV. Difficulties like limited γ -ray event statistics coupled with rather large error bars do not allow us to claim the cutoff feature at a high confidence level. Keeping in view that the cutoff energy $E_0 = (4.7 \pm 2.1)TeV$ inferred from our observations is fairly consistent with the cutoff values of $3.6(+0.4 - 0.3)_{stat}(+0.9 - 0.8)_{sys}TeV$ and $(4.3 \pm 0.3)TeV$ reported by the HEGRA [11] and the VERITAS [16] groups, respectively, it seems necessary to improve upon our analysis procedure so that the claim can be put on a firmer basis. Furthermore, the results of the HESS group [7], based on 9 nights in Apr. and May 2004, also indicate that the time averaged energy spectrum of Mrk 421 is well described by a power law with index $\Gamma = 2.1 \pm 0.1_{stat} \pm 0.3_{sys}$ with an exponential cutoff at $3.1(+0.5 - 0.4)_{stat} \pm 0.9_{sys}TeV$. The HESS results also indicate that the cutoff signature in the energy spectrum is intrinsic to the source.

In conclusion, we believe that, despite the limited sensitivity of the TACTIC telescope, the TeV light curve presented here, for nearly 5 months of extensive observations, should provide a useful input for the γ -ray astronomy community. Furthermore, we also believe that there is considerable scope for a TACTIC like imaging telescope for monitoring AGNs on a long term basis.

8 Acknowledgements

The authors would like to convey their gratitude to all the concerned colleagues of the Astrophysical Sciences Division for their contributions towards the instrumentation and observation aspects of the TACTIC telescope. We would also like to thank the anonymous referees for making several helpful suggestions.

References

- [1] M.Punch, et al., Nature, 358 (1992) 477.
- [2] D.Petry et al., A&A, 311 (1996) L13.
- [3] J.A.Zweerink et al., ApJ, 490(1997) L144.
- [4] F.Piron et al., A&A, 374 (2001) 895.
- [5] F.Aharonian et al., A&A, 410 (2003)813.
- [6] L.M.Boone et al., ApJ, 579 (2002) L8.
- [7] F.Aharonian et al., A&A, 437(2005) 95.

- [8] J.Albert et al., submitted to ApJ, (2006)
- [9] D.A.Smith et al., A&A, 459 (2006) 453.
- [10] J.A.Gaidos et al., Nature, 383(1996) 319.
- [11] F.Aharonian et al., A&A, 393 (2002) 89.
- [12] H.Buckley et al., ApJ, 472 (1996) L9.
- [13] T.Takahashi et al., ApJ, 470 (1996) L89.
- [14] T.Takahashi et al., ApJ, 542(2000) L105.
- [15] H.Blazewski et al., ApJ, 630 (2005) 130.
- [16] F.Krennrich et al., ApJ, 575 (2002) L9.
- [17] E.Dwek & F.Krennrich, ApJ, 618 (2005) 657.
- [18] R.A.Ong, Proc. 29th ICRC (Pune) , 10 (2005)329.
- [19] S.R.Kaul et al., Nucl. Instrum. and Meth. A., 496 (2003) 400.
- [20] N.Bhatt et al., Meas. Sci. Technol., 12 (2001) 167.
- [21] K.K.Yadav et al., Nucl. Instrum. and Meth. A., 527 (2004) 411.
- [22] S.Thoudam et al., Proc. 29th ICRC (Pune), 4 (2005) 363.
- [23] S.V.Godambe et al., Proc. 29th ICRC (Pune), 4 (2005)347.
- [24] R.C.Rannot et al., Proc. 29th ICRC (Pune), 4(2005) 355.
- [25] A.Konopelko et al., Astropart. Phys., 4 (1996)199.
- [26] A.M.Hillas, Proc. 19th ICRC (La Jolla), 3 (1985) 445.
- [27] T.C.Weekes et al., ApJ, 342 (1989) 379.
- [28] G.Mohanty et al., Astropart. Phys., 9 (1998)15.
- [29] M.Catanese et al., ApJ, 501 (1998) 616.
- [30] T.P.Li & Y.Q.Ma, ApJ, 272 (1983) 317.
- [31] <http://xte.mit.edu/>
- [32] D.Heck et al., Report FZKA 6019 Forschungszentrum, Karlsruhe, (1998).
- [33] A.K.Tickoo et al., Nucl. Instrum. and Meth. A., 539 (2005) 177.
- [34] P.T.Reynolds and D.J.Fegan, Astropart. Phys., 3 (1995)137.
- [35] M.J.Lang, J.Phys.G : Nucl. Part. Phys., 24 (1998) 2279.
- [36] M. Reidmiller, Computer Standards Interfaces, 16 (1994) 265.
- [37] A.M.Hillas et al., ApJ, 503 (1998) 744.
- [38] F.Aharonian et al., ApJ, 614 (2004) 897.
- [39] <http://veritas.sao.arizona.edu/>